Electronic Supplementary Information

Lanthanides SMM with cationic and anionic complex fragments formed by the Schiff base: structure, luminescence, magnetic properties and ab initio calculations

Alexey Gusev, Ivan Nemec, Radovan Herchel, Yuriy Baluda, Konstantin Babeshkin, Nikolay Efimov, Mikhail Kiskin, Wolfgang Linert

Contents

Table S8	The splitting of the lowest multiplets for Dy-anionic complex of 3 calculated by CASSCF/SINGLE_ANISO (method B) together with g-values for each Kramers doublets

Table S1. Crystal data and structure refinement summary for complexes 1-3

	1	2	3
Crystal data			
Crystal system, space group	Monoclinic, *P*2/*n*	Monoclinic, *P*2/*n*	Monoclinic, *P*2/*n*
Temperature (K)	150	150	150
a, (Å) *b*, (Å) *c* (Å)	17.561 (5), 10.410 (3), 24.663 (10)	17.603 (12), 10.429 (10), 24.755 (14)	17.539 (2), 10.4381 (10), 24.728 (2)
β (°)	106.452 (14)	106.180 (16)	106.211 (4)
V (Å^3)	4324 (2)	4365 (6)	4347.0 (8)
Z	2	2	2
Radiation type	Mo *K*α	Mo *K*α	Mo *K*α
μ (mm^{-1})	1.60	1.68	1.78
Crystal size (mm)	0.1 × 0.06 × 0.02	0.10 × 0.06 × 0.02	0.15 × 0.12 × 0.05
No. of measured, independent and observed [$I > 2\sigma(I)$] reflections	41651, 10314, 7515	45284, 10824, 7520	52297, 13408, 10405
R_{int}	0.077	0.093	0.050
$(\sin\theta/\lambda)_{max}$ (Å^{-1})	0.658	0.667	0.720
No. of reflections	10314	10824	13408
No. of parameters	559	559	557
No. of restraints	21	21	4

Table S2. Selected bond length for complexes 1-3.

1		**2**		**3**	
Bond	Length, Å	Bond	Length, Å	Bond	Length, Å
Gd1—O5	2.401 (3)	Tb1—O3	2.288 (4)	Dy1—O2^{i}	2.289 (2)
Gd1—O5^{i}	2.402 (3)	Tb1—O3^{i}	2.288 (4)	Dy1—O2	2.289 (2)
Gd1—O3	2.299 (4)	Tb1—O5	2.389 (4)	Dy1—O1	2.314 (2)
Gd1—O3^{i}	2.299 (4)	Tb1—O5^{i}	2.389 (4)	Dy1—O1^{i}	2.314 (2)
Gd1—O4^{i}	2.410 (4)	Tb1—O4	2.411 (4)	Dy1—N3	2.557 (3)
Gd1—O4	2.410 (4)	Tb1—O4^{i}	2.411 (4)	Dy1—N3^{i}	2.557 (3)
Gd1—N9	2.556 (4)	Tb1—N9^{i}	2.555 (4)	Dy1—N4	2.589 (3)
Gd1—N9^{i}	2.556 (4)	Tb1—N9	2.555 (4)	Dy1—N4^{i}	2.589 (3)
Gd2—O1^{ii}	2.329 (3)	Tb2—O2^{ii}	2.302 (4)	Dy2—O3	2.276 (3)
Gd2—O1	2.329 (3)	Tb2—O2	2.302 (4)	Dy2—O3^{ii}	2.276 (3)
Gd2—O2	2.314 (3)	Tb2—O1^{ii}	2.322 (4)	Dy2—O5^{ii}	2.372 (2)
Gd2—O2^{ii}	2.314 (3)	Tb2—O1	2.322 (4)	Dy2—O5	2.372 (2)
Gd2—N4^{ii}	2.592 (4)	Tb2—N3^{ii}	2.567 (4)	Dy2—O4	2.411 (2)
Gd2—N4	2.592 (4)	Tb2—N3	2.567 (4)	Dy2—O4^{ii}	2.411 (2)
Gd2—N3^{ii}	2.564 (4)	Tb2—N4	2.600 (4)	Dy2—N9^{ii}	2.544 (3)
Gd2—N3	2.564 (4)	Tb2—N4^{ii}	2.600 (4)	Dy2—N9	2.544 (3)

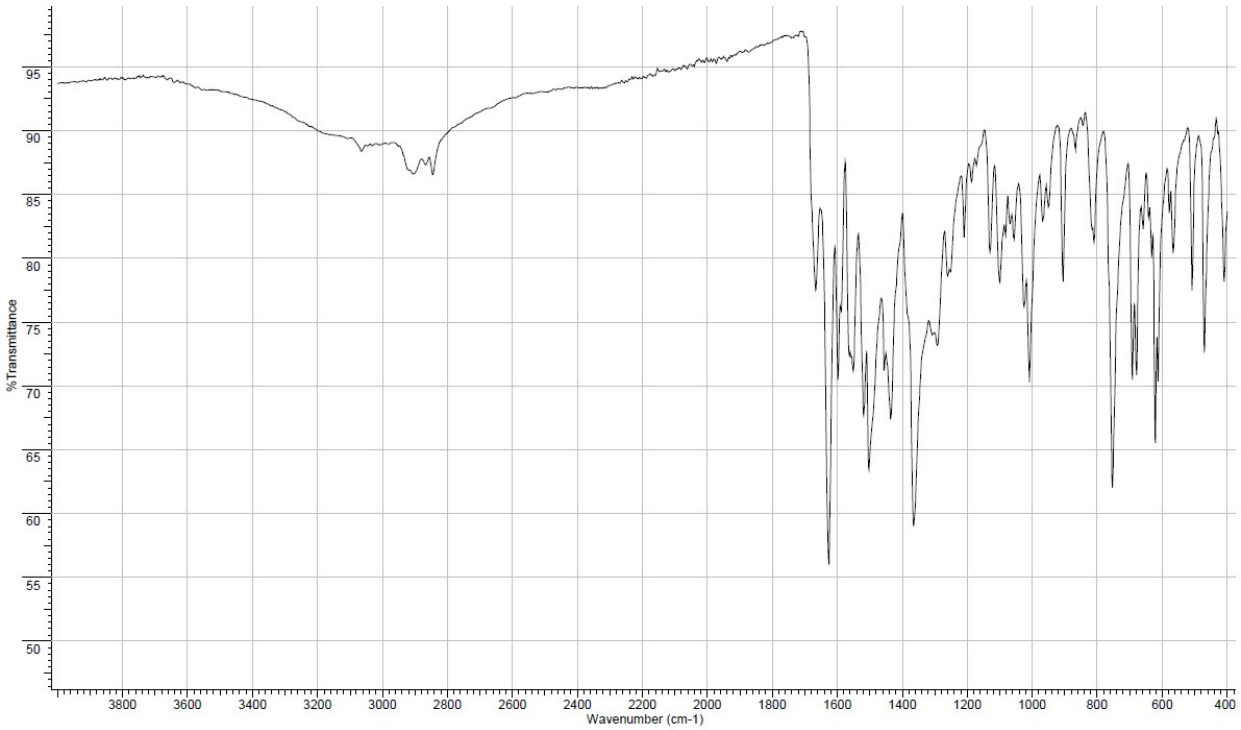

Figure S1. IR spectra of complex 1.

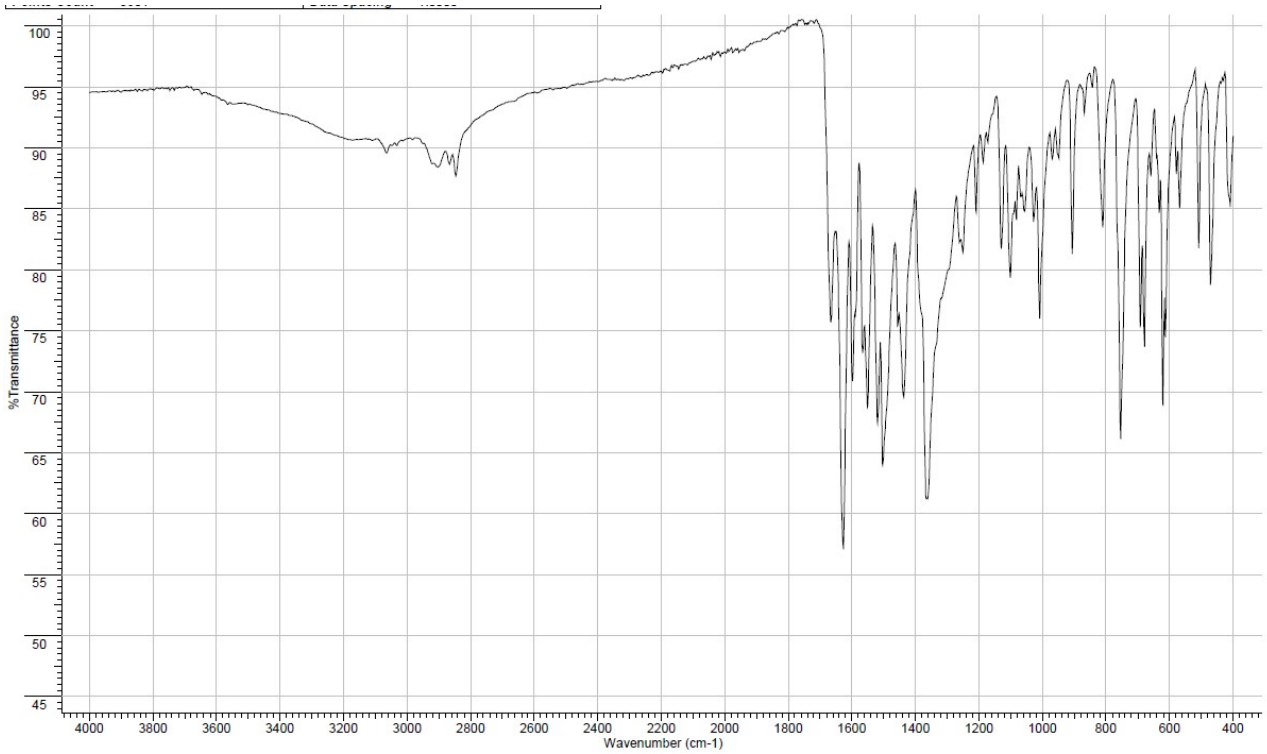

Figure S2. IR spectra of complex 2.

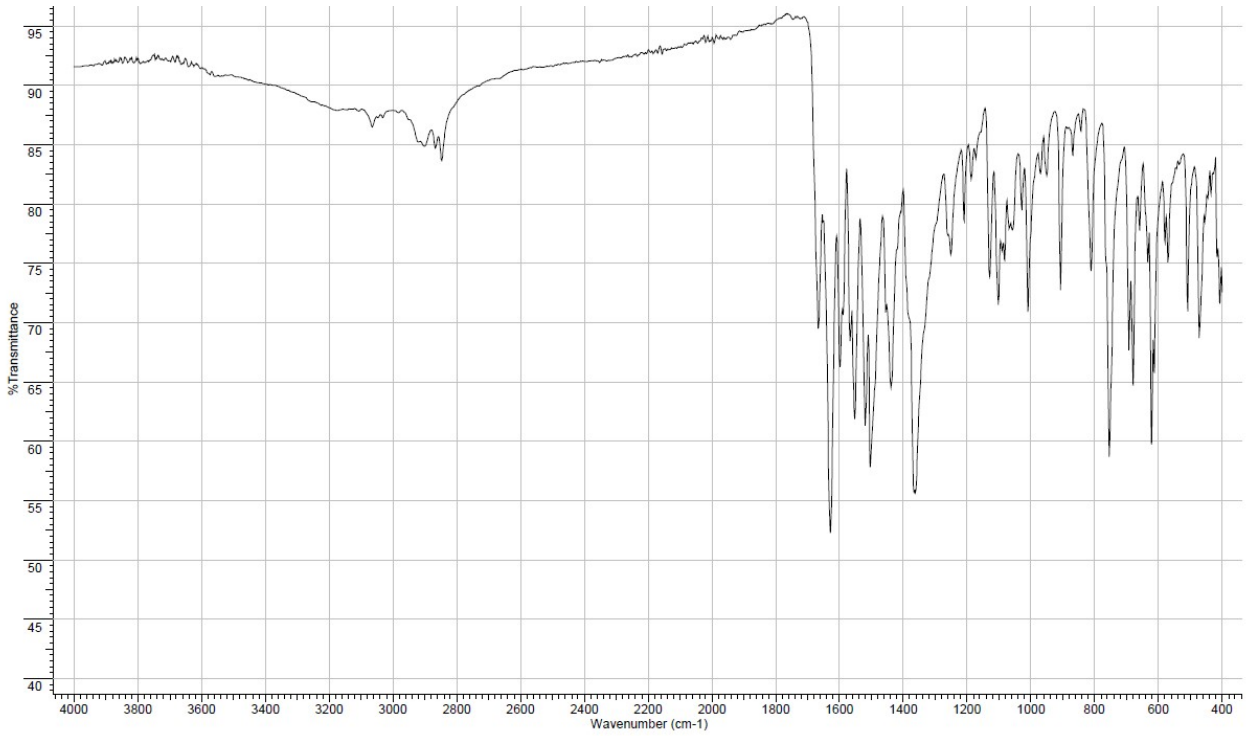

Figure S3. IR spectra of complex 3.

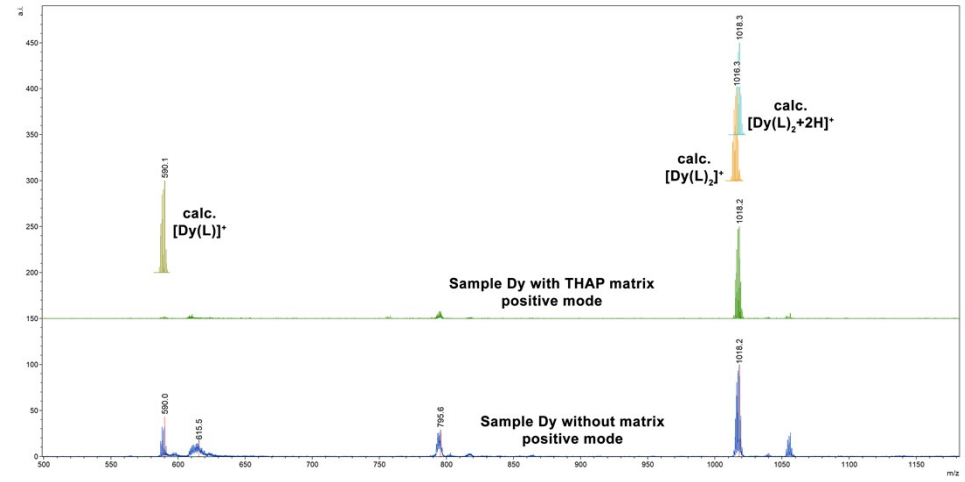

a)

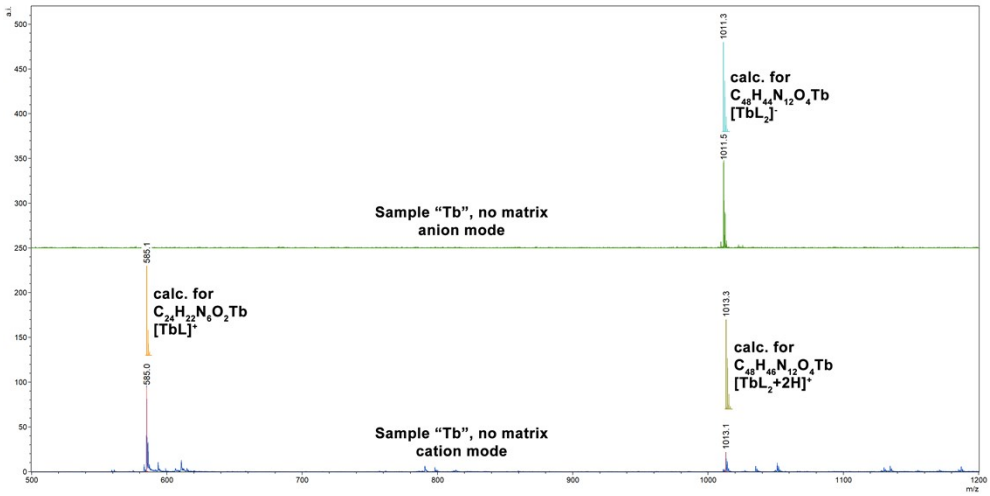

b)

Figure S4. a) ESI-MS spectra of complex 3; b) ESI-MS spectra of complex 2.

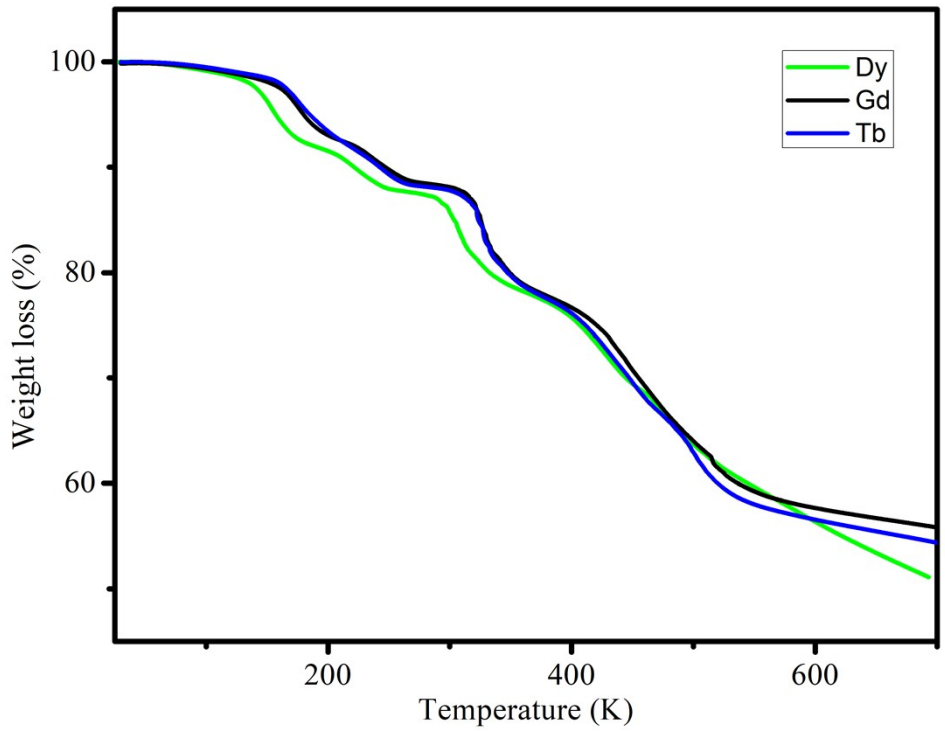

Figure S5. TG curves of complexes 1-3.

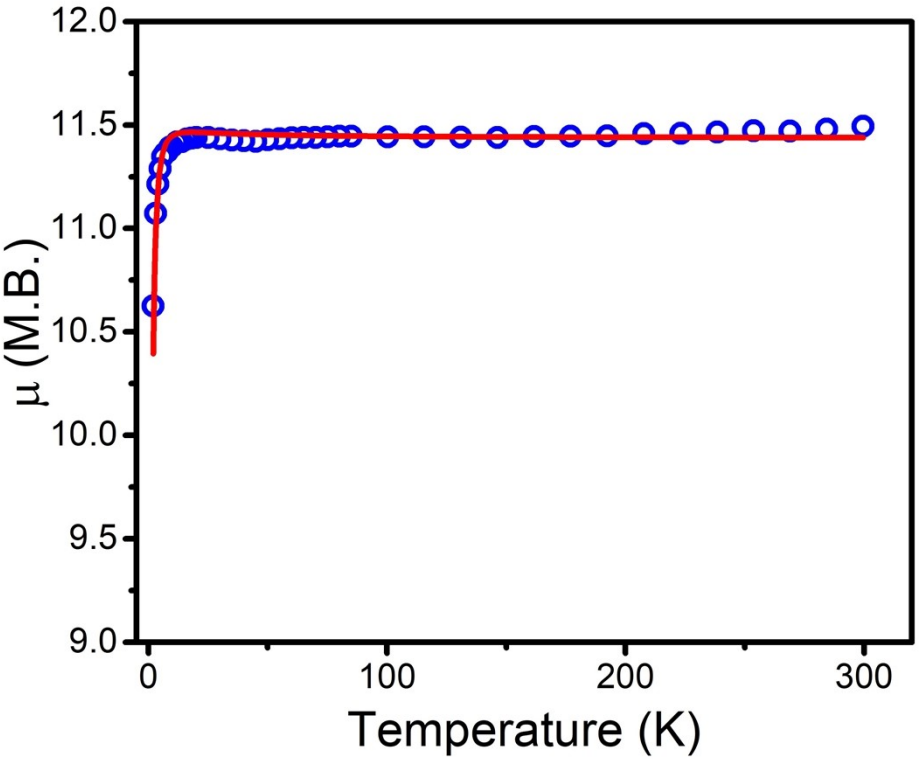

Figure S6. Temperature dependence of magnetic moment for 1. The red lines represent the best fit of the

theoretical model described in the main text.

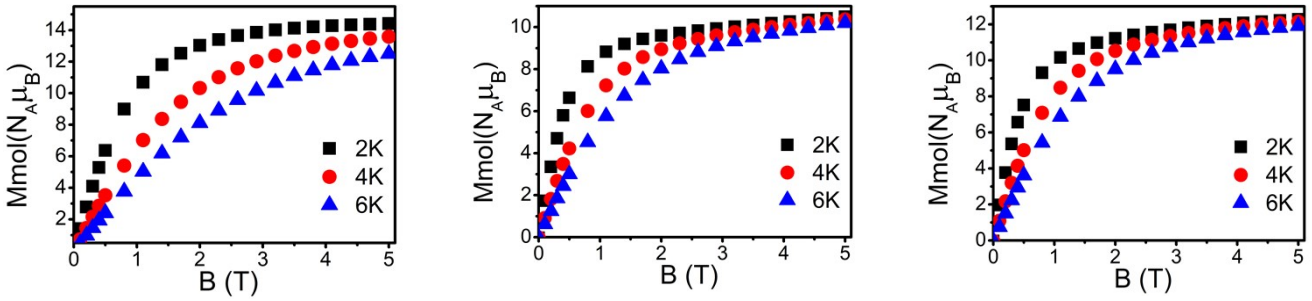

Figure S7. Field dependence of molar magnetization for **1** (a), **2** (b) and **3** (c) at different temperatures.

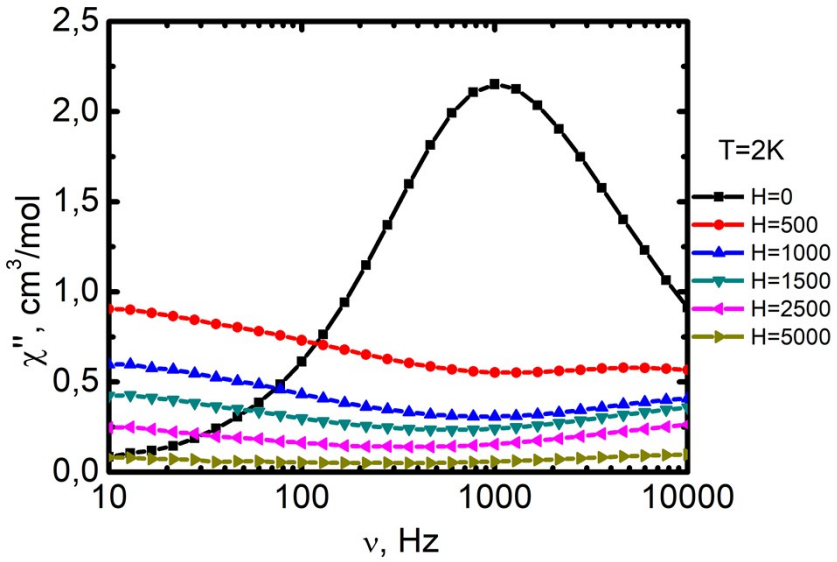

Figure S8. Field dependence of the out-of-phase signal vs frequency at 2 K for **3**

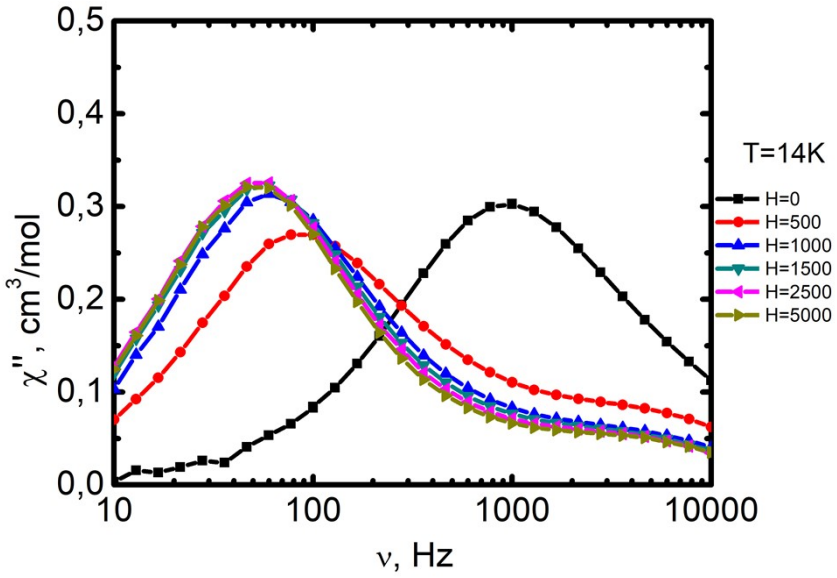

Figure S9. Field dependence of the out-of-phase signal vs frequency at 14 K for **3**

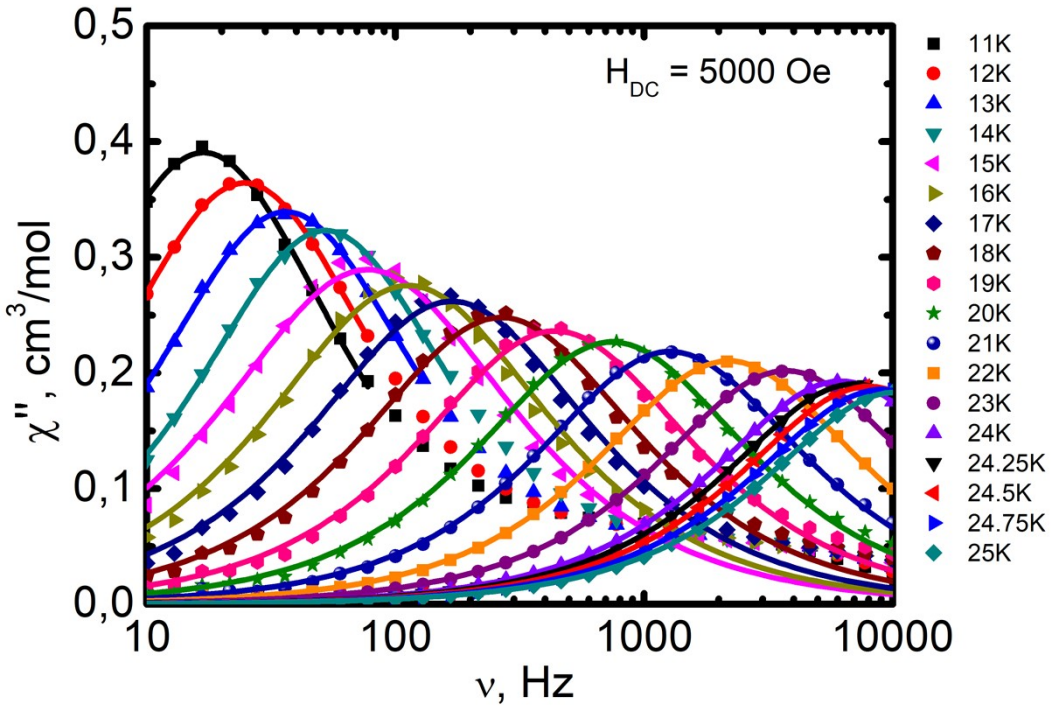

Figure S10. Frequency dependence of the out-phase χ'' ac susceptibility signals for **3** under 5000 Oe dc field

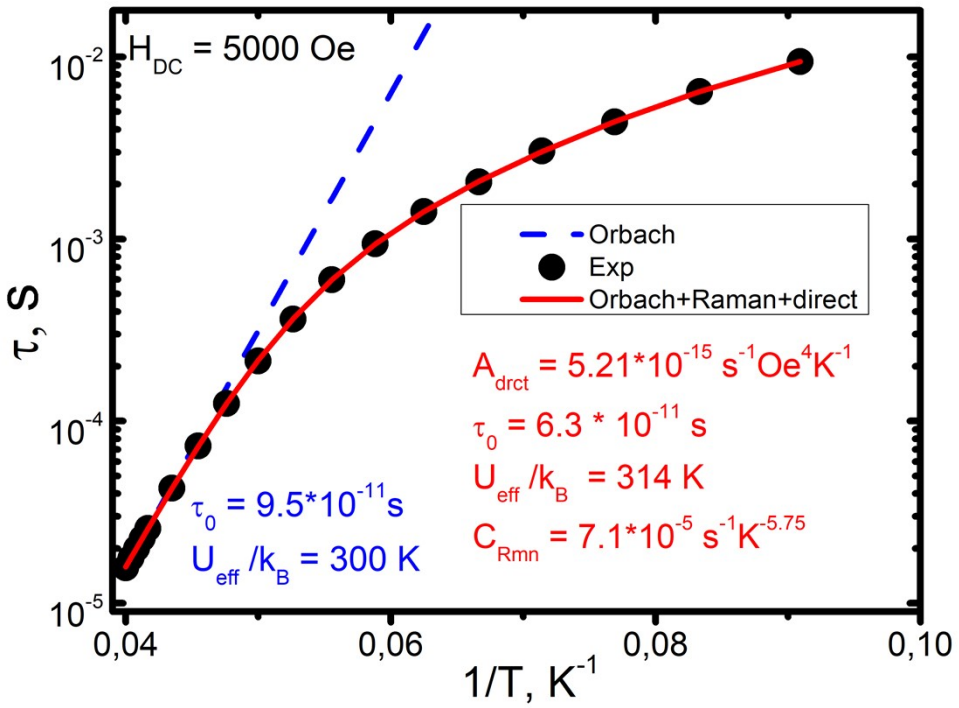

Figure S11. Relaxation data at 5000 Oe plotted as τ vs. T^{-1} for **3**. The lines represent the best fits of experimental data to the Arrhenius equation and multiple relaxation processes

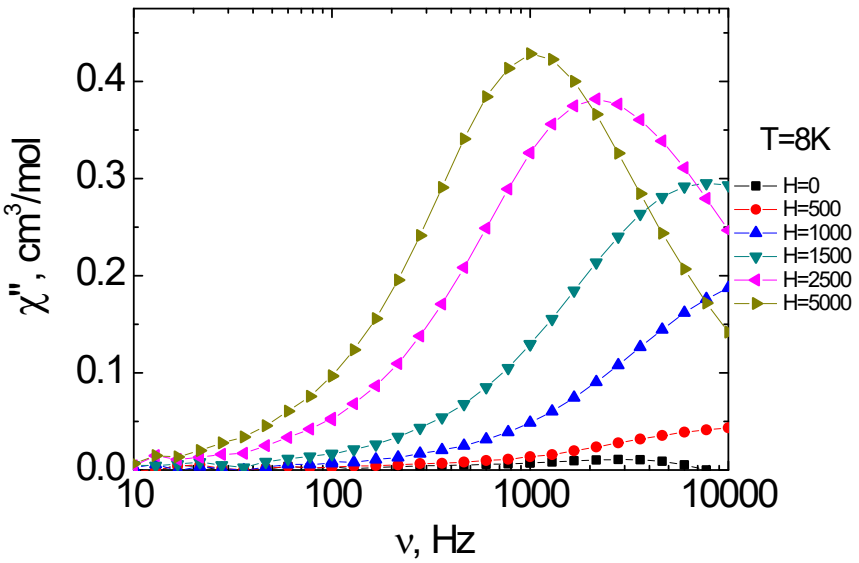

Figure S12. Field dependence of the out-of-phase signal vs frequency at 8 K for **2**

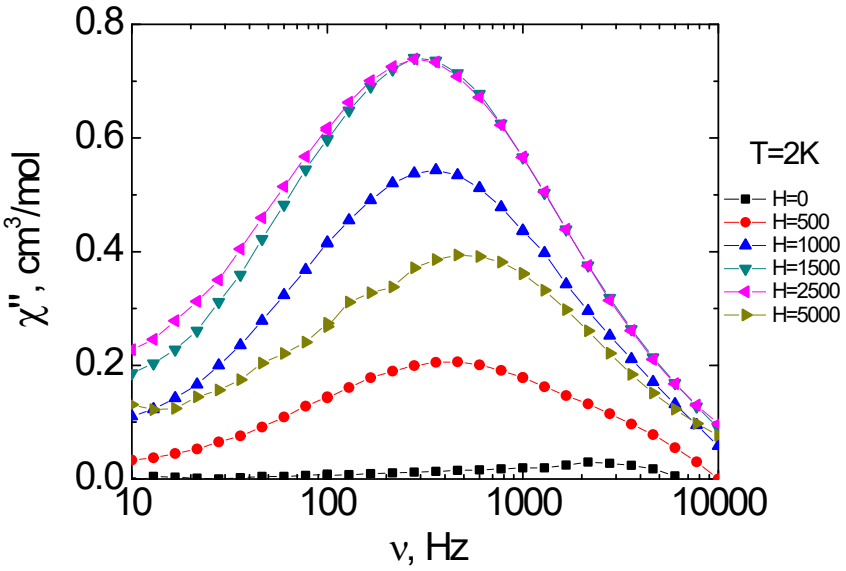

Figure S13. Field dependence of the out-of-phase signal vs frequency at 2 K for **1**

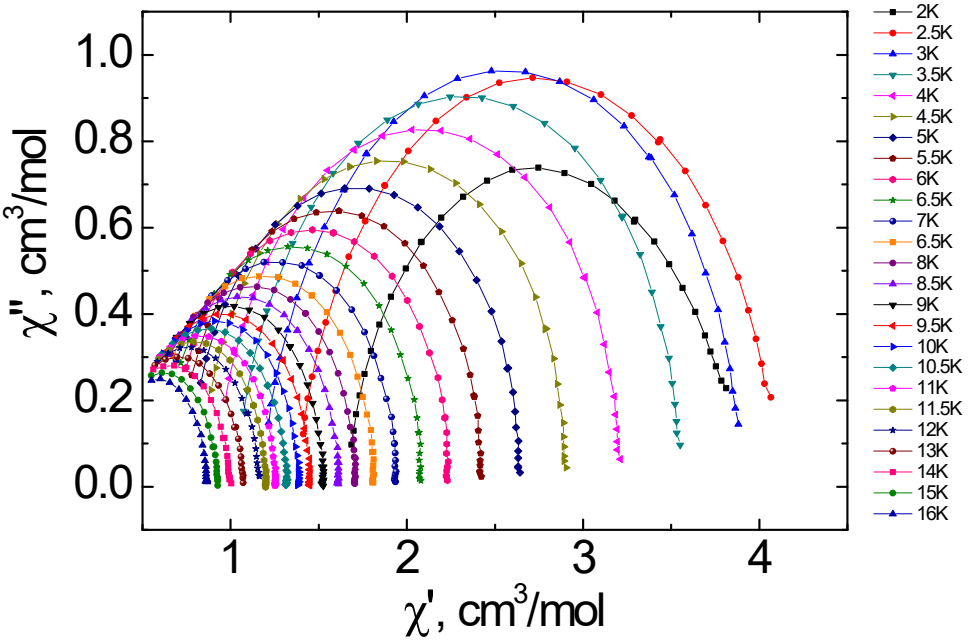

Figure S14. Cole-Cole dependence for **1** at different temperatures under 2500 Oe dc-field.

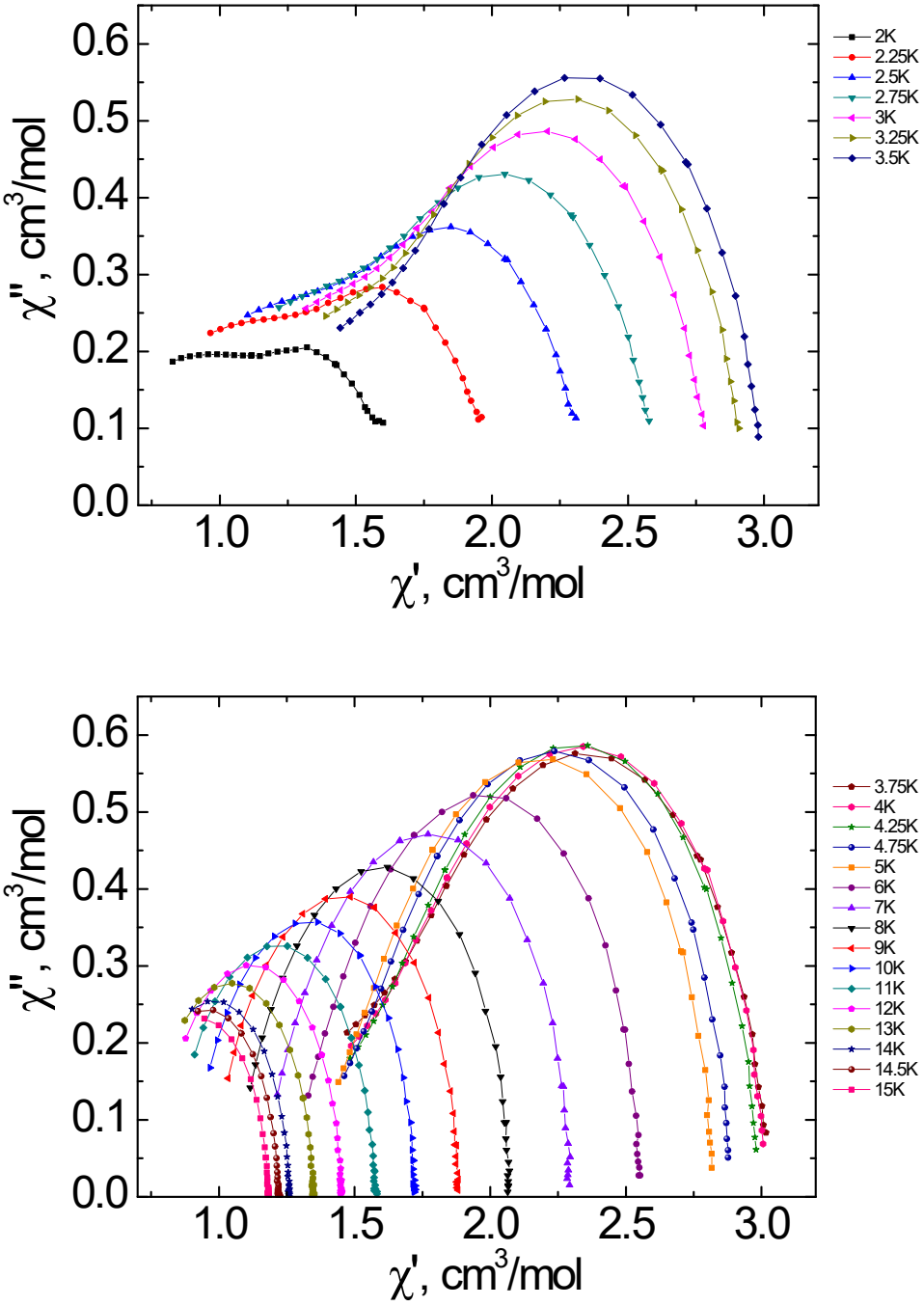

Figure S15. Cole-Cole dependence for **2** at different temperatures under 5000 Oe dc-field.

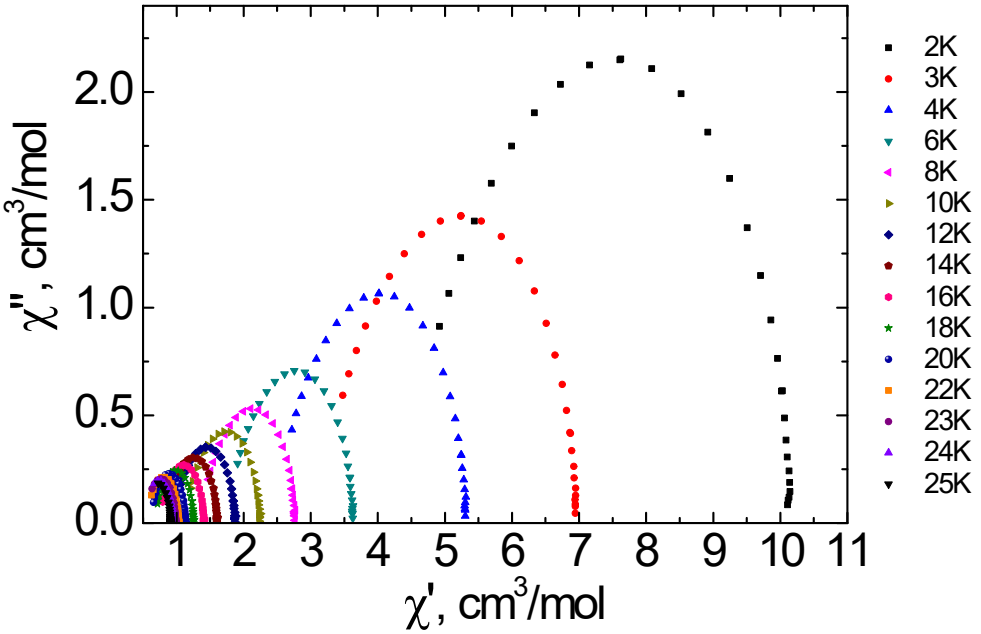

Figure S16. Cole-Cole dependence for **3** at different temperatures under zero dc-field.

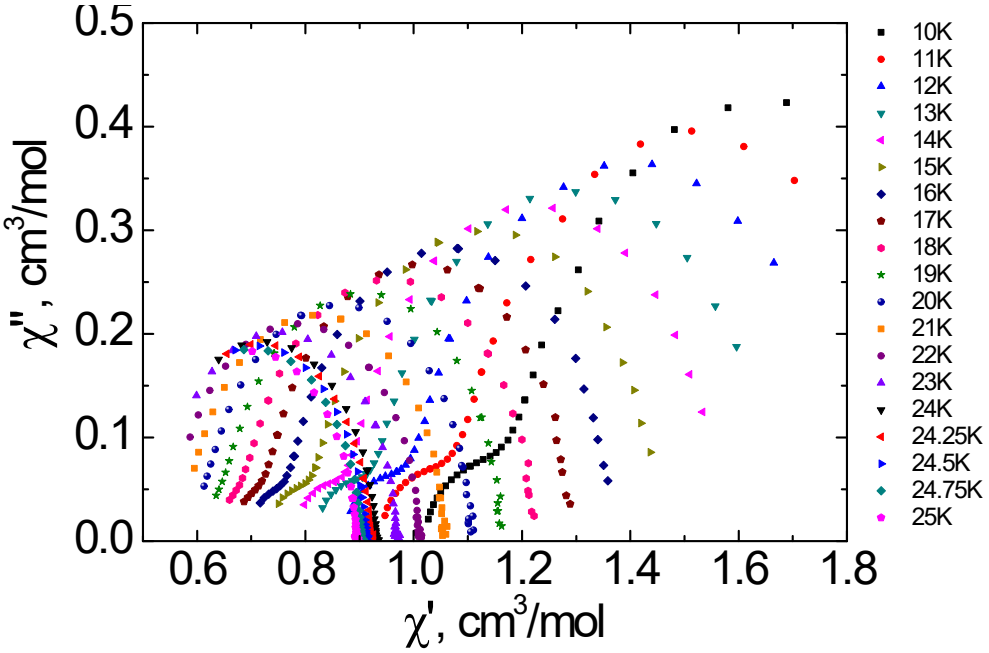

Figure S17. Cole-Cole dependence for **3** at different temperatures under 5000 Oe dc-field.

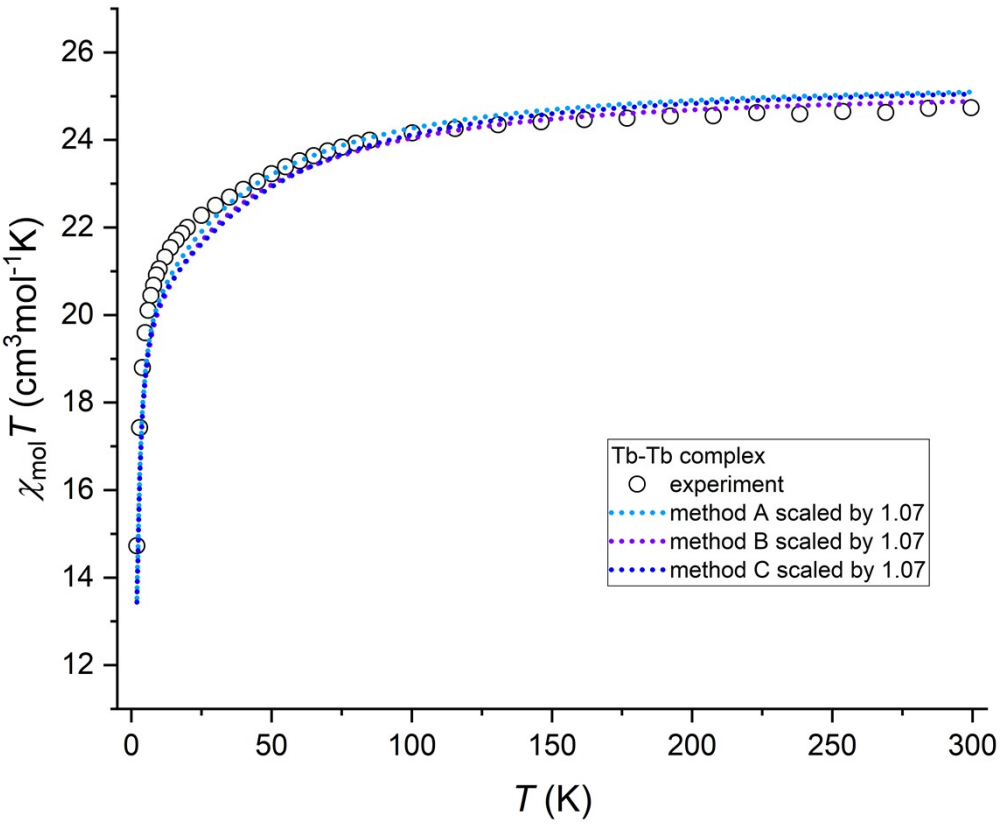

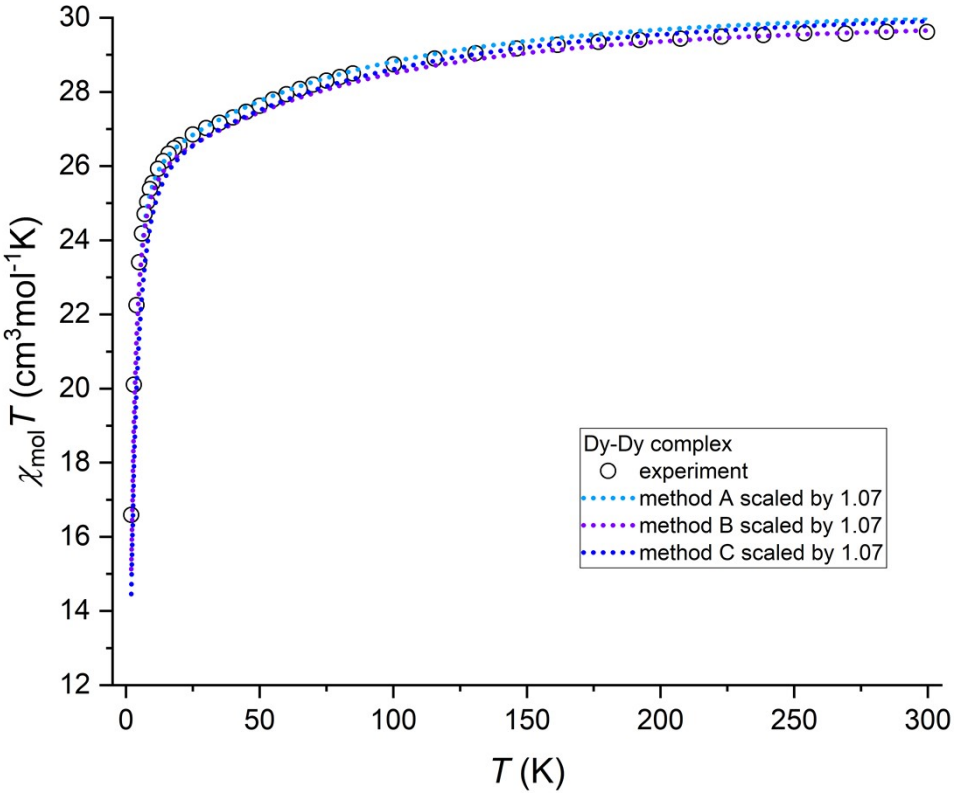

Figure 18. The comparison of the experimental magnetic data for **2** and **3**, and the calculated data from CASSCF/(NEVPT2/SINGLE_ANISO calculations (method A-C).

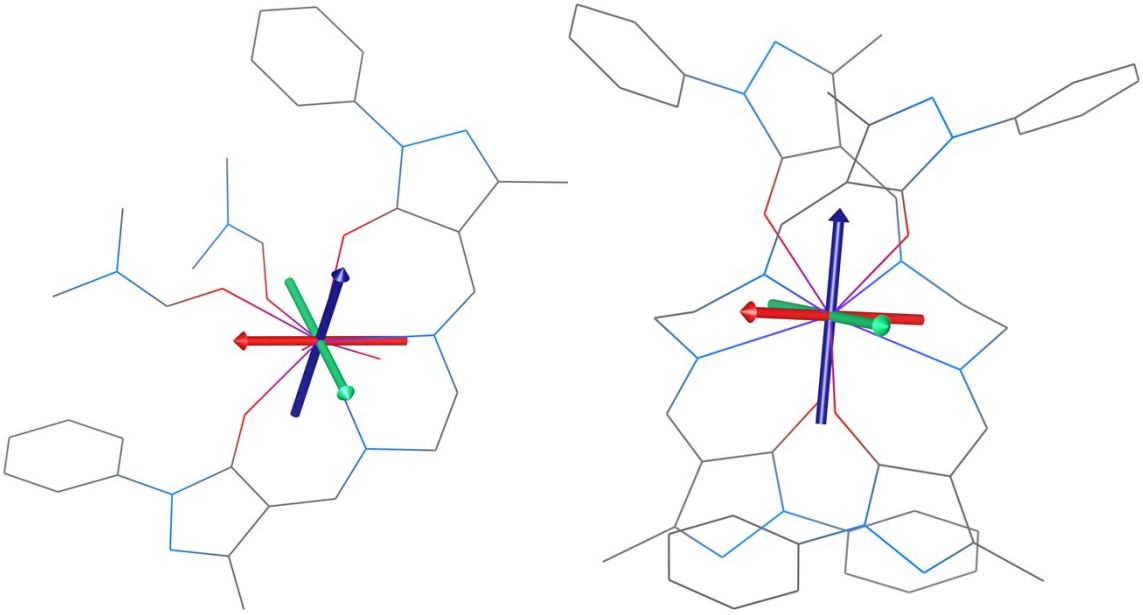

Figure S19. The molecular structures of complex cation (top) and anion (bottom) of compound **2** overlaid with principal axis of g-tensor of the first pseudo doublet (x/y/z-axes colored as red/green/blue arrows) resulting from CASSCF/SINLGE_ANISO (method B).

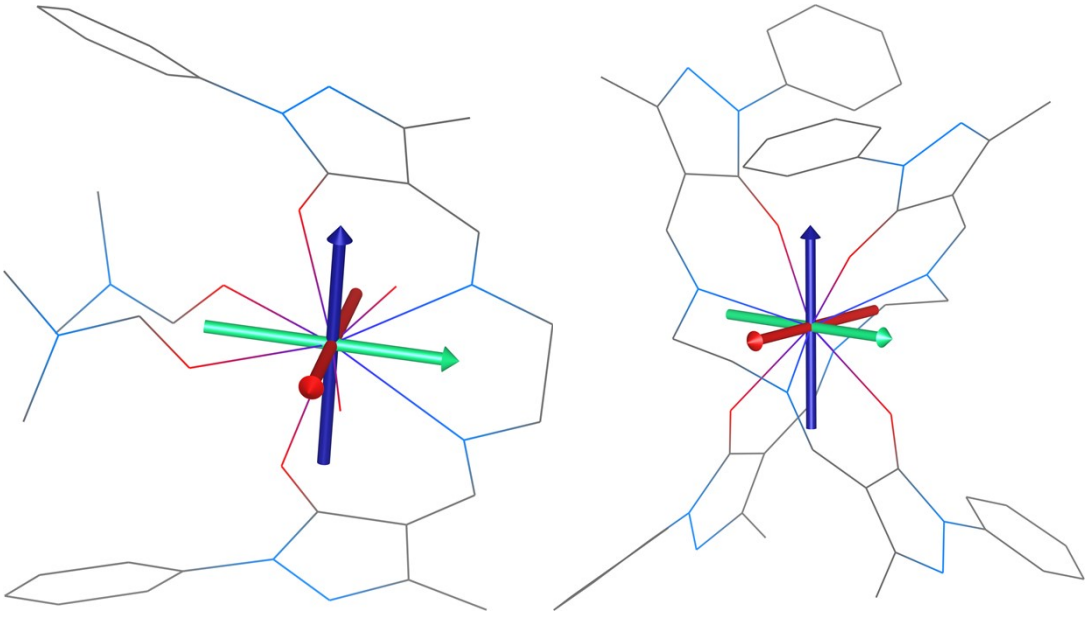

Figure S20. The molecular structures of complex cation and anion of compound **3** overlaid with principal axis of g-tensor of the first Kramers doublet (x/y/z-axes colored as red/green/blue arrows) resulting from CASSCF/SINLGE_ANISO (method B).

Table S3. The summarization of SMMs on Dy(III) ion and Salen-type ligand basis.

Complex	$\Delta E/k_B$ (K)	Ref
$[Dy_4(L1)_2(HL_1)_2Cl_2(OH)_2]_2Cl_2(OH)_2 3EtOH \cdot H_2O$	55,71	1
$[Dy_4(L1)_6] \cdot 5.5H_2O$	17.2	2
$[Dy_4(L2)_4(\mu 3\text{-}O)_2(NO_3)_2]$	68.59	3
$[Ln(H_2L3)(NO_3)_3]$	44.6	4
$\{Dy(H_2L4)\ 1.5(NO_3)_3] \cdot 5CHCl_3 \cdot CH_3OH\}$	20.24	5
$(Et_3NH)[Dy((R,R)/(S,S)\text{-}L5)_2]$	39.9	6
$[Dy(L6)(NO_3)(CH_3OH)_2]$	157.78	7
$(Et_3NH)[Dy(L7)_2]$	39.7	8
$[Dy_4(L2)_2(HL8)_2(NO_3)_2(OH)_2](NO_3)_2\ 4H_2O$	48.1	9
$[Dy(H_2L8)_{1.5}Cl_3]n$	24.4 K	10
$[Dy_2(H_2L8)_2(NO_3)_4(CH_3O)_2]_n$	50.9	11
[Dy4(HL6)4(OAc)2(H2O)2]·2Et3NH·2CH3CN	207(2) 343	12
$[Dy(H_2O)_2(DMF)_2L][DyL_2]$	243 (H = 0 Oe) 314 (H = 5000 Oe)	This work

H_2L1 - N,N'-bis(salicylidene)-1,2-ethylendiamine
H_2L2- N,N'-bis(3-methoxysalicylidene)cyclohexane-1,2-diamine
H_2L3-N,N'-bis(3-methoxysalicylidene)- 2,2-dimethylbutanediamine-1,3
H_2L4 - N,N'-bis(salicylidene)-1,2-cyclohexanediamine
H_2L5 -N,N'-(1,2-cyclohexanediylethylene)bis(3-nitrosalicylideneiminato
H_2L6 - N,N'-bis(5-nitrosalicylaldehyde)ethane-1,2-cyclohexanediamine
H_2L7 - N,N'-bis(3-nitro-salicylaldene)ethylenediamine
H_2L8 - N,N'-bis(salicylidene)-1,4-butanediamine

(1) F. Luan, T. Liu, P. Yan, X. Zou, Y. Li, and G. Li, Inorg. Chem. 2015, 54, 7, 3485–3490;
(2) B. H. Koo, K. S. Lim, D. W.Ryu, W. R. Lee, E. K. Koh, C. S. Hong, Dalton Trans., 2013,42, 7204-7209;
(3) Z.-H. Zhu, H.-F. Wang, S. Yu, H.-H. Zou, H.-L. Wang, B. Yin, F.-P. Liang, Inorg. Chem. 2020, 59, 16, 11640–11650;
(4) L. Hua , F.-W. Zheng , H.-T. Chen, L. Wang, D.-J. Li, L. Yang, F.-J. Han, X.-Y. Duan , T.-T. Liu , W.-X. Wang, Journal of Solid State Chemistry 2021, 303, 122463;
(5) X. Zou, C. Du, Y. Dong, G. Li, Inorganica Chimica Acta 2020, 507, 119455;
(6) M. Ren, Z.-L. Xu, T.-T. Wang, S.-S. Bao, Z.-H. Zheng, Z.-C. Zhang, L.-M. Zheng. Dalton Trans., 2016, 45, 690-695;
(7) L. Wang, X. Yao, X. Zou, J. Li, W. Sun, G. Li, CrystEngComm, 2022,24, 1907-1916;
(8) M. Ren, Z.-L. Xu, S.-S. Bao, T.-T. Wang, Z.-H. Zheng, R. A. S. Ferreira, L.-M. Zheng, L. D. Carlos, Dalton Trans., 2016, 45, 2974-2982; (9) F. Luan, P. Yan, J. Zhu, T. Liu, X. Zoua, G. Li, Dalton Trans., 2015,44, 4046-4053;
(10) Y. Yue, G. Hou, X. Yao, G. Li, Polyhedron, 2017, 129, 157-163;
(11) Y. Yue, P. Yan, J. Sun, G. Li, Inorganic Chemistry Communications, 2015, 54, 5–8

Table S4. The summarization of SMMs on Dy(III) ion and Schiff base ligand basis with $\Delta E/k_B$.>200 K

Complex	$\Delta E/k_B$ (K)	Ref
$[Dy(L1)_2(THF)_2][B(C_6H_5)_4]$	378 (H = 0 Oe)	1
$[Dy(L2)_2(Py)_2][B(C_6H_5)_4]$	388 (H = 0 Oe)	1
$Dy(HL3)_3$	270 (H = 1000 Oe) Magnetically diluted	2
$[Dy_4(L4)_2(HL4)_2(N_3)_4(O)]\cdot 14H_2O$	270 (H = 1600 Oe)	3
$\{Dy_2(L5)_2(Phen)_2(diphenylphosphate)_2(MeOH)_2\}$	232.9 (H = 0 Oe)	4
$[Dy_4(HL6)_4(OAc)_2(H_2O)2]\cdot 2Et_3NH\cdot 2CH_3CN$	207 and 343 (H = 0 Oe)	5
$[Dy(L7)_2(py)_2][B(Ph)_4]\cdot py$	679 (H = 0 Oe)	6
$[Dy(H_2O)_2(DMF)_2L][DyL_2]$	243 (H = 0 Oe) 314 (H = 5000 Oe)	This work

L1 - 2,4-di-tert-butyl-6-((quinolin-8-ylimino)methyl)phenolate
L2- 2,4-di-tert-butyl-6-(((pyridin-2-ylmethyl)imino)methyl)phenolate
H_2L3-2-hydroxy-N'-[(E)-(2-hydroxy-3-methoxyphenyl)methylidene]benzhydrazide
H_2L4 1,3-bis[1-(2-pyridyl)ethylideneamino]urea
H_2L5 - 2-(((2-hydroxyphenyl)imino)methyl)-6-methoxyphenol
H_2L6 - N,N'-bis(3-hydroxylsalicylidene)benzene-1,2-diamine
L7 - 2,4-bis(1,1-dimethylethyl)-6-[[(2-methoxy-5-methylphenyl)imino]methyl] phenolate

(1) J. Long, I. Basalov, N. Forosenko, K. A. Lyssenko, E. Mamontova, et al.. Chemistry-A European Journal, 2019, 25 (2), 474-478.doi10.1002/chem.201804429;

(2) Eva Lucaccini, Matteo Briganti, Mauro Perfetti, Laure Vendier, Jean-Pierre Costes, Federico Totti, Roberta Sessoli, and L. Sorace. Chem. Eur. J. 2016, 22, 5552 – 5562

(3) M. U. Anwar, L. K. Thompson, L. N. Dawe, F. Habib, M. Murugesu Chem. Commun., 2012, 48, 4576–4578

(4) S. P. Bera, A. Mondal, S. Konar, Inorg. Chem. Front., 2020, 7, 3352-3363

(5) T.-T. Wang, Z.-W. Che, J.-T. Chen, H. Yan, T.-D. Zhou, Y.-Q. Zhang, W.-B. Sun. Inorg. Chem. Front., 2023, 10, 1501–1510

(6) J. Long, I. V. Basalov, K. A. Lyssenko, A. V. Cherkasov, E. Mamontova, Y. Guari, J. Larionova, A. A. Trifonov. Chem. Asian J., 2020, 15, 2706-2715

Table S5. The splitting of the lowest multiplets for Tb-cationic complex of **2** calculated by CASSCF/SINGLE_ANISO (method B) together with g-values for selected pseudo doublets and respective tunnelling rates

E (cm^{-1})	
0	$g_x = 0.000$, $g_y = 0.000$, $g_z = 16.540$, $\Delta_{tun} = 0.784$ cm^{-1}
0.8	
61.5	$g_x = 0.000$, $g_y = 0.000$, $g_z = 12.597$, $\Delta_{tun} = 2.261$ cm^{-1}
63.8	
67.3	$g_x = 0.000$, $g_y = 0.000$, $g_z = 15.852$, $\Delta_{tun} = 0.863$ cm^{-1}
68.2	
124	
145	
185	
308	
316	
635	
636	

Table S6. The splitting of the lowest multiplets for Tb-anionic complex of **2** calculated by CASSCF/SINGLE_ANISO (method B) together with g-values for selected pseudo doublets and respective tunnelling rates

E (cm^{-1})	
0	$g_x = 0.000$, $g_y = 0.000$, $g_z = 17.783$, $\Delta_{tun} = 0.007$ cm^{-1}
0	
161	$g_x = 0.000$, $g_y = 0.000$, $g_z = 17.792$, $\Delta_{tun} = 0.154$ cm^{-1}
161	
174	$g_x = 0.000$, $g_y = 0.000$, $g_z = 14.319$, $\Delta_{tun} = 0.832$ cm^{-1}
175	
285	
292	
309	
323	
346	
439	
442	

Table S7. The splitting of the lowest multiplets for Dy-cationic complex of **3** calculated by CASSCF/SINGLE_ANISO (method B) together with g-values for each Kramers doublets

E (cm^{-1})	g_x	g_y	g_z
0	0.003	0.004	19.617
201	0.201	0.352	16.355
324	3.055	4.921	13.821
387	7.052	5.262	0.349
481	3.086	3.560	10.706
552	0.213	0.397	15.531
639	0.004	0.051	19.216
706	0.001	0.009	19.778

Table S8. The splitting of the lowest multiplets for Dy-anionic complex of **3** calculated by CASSCF/SINGLE_ANISO (method B) together with g-values for each Kramers doublets

E (cm^{-1})	g_x	g_y	g_z
0	0.617	5.253	13.584
5.8	0.693	4.568	13.453
118	2.569	4.354	14.826
161	8.672	6.374	0.402
255	8.474	7.589	0.210
325	8.887	6.768	2.792
346	2.342	3.394	7.652
378	11.996	7.872	0.690